CHIN. PHYS. LETT. Vol. 33, No. 10 (2016) 106401

Strain Avalanches in Microsized Single Crystals: Avalanche Size Predicted by a Continuum Crystal Plasticity Model *

Xu Zhang(张旭)[1,2**], Xiang-Cheng Zhang(张香成)[1], Qian Li(李倩)[1], Fu-Lin Shang(尚福林)[2]

[1]*National Center for International Joint Research of Micro-nano Moulding Technology, School of Mechanics and Engineering Science, Zhengzhou University, Zhengzhou 450001*

[2]*State Key Laboratory for Strength and Vibration of Mechanical Structures, School of Aerospace, Xi'an Jiaotong University, Xi'an 710049*

(Received 4 July 2016)

Plastic deformation of small crystals occurs by power-law distributed strain avalanches whose universality is still debated. In this work we introduce a continuum crystal plasticity model for the deformation of microsized single crystals, which is able to reproduce the main experimental observations such as flow intermittency and statistics of strain avalanches. We report exact predictions for scaling exponents and scaling functions associated with random distribution of avalanche sizes. In this way, the developed model provides a routine for a quantitative characterization of the statistical aspects of strain avalanches in microsized single crystals.

PACS: 64.60.av, 62.20.fq, 62.20.F− DOI: 10.1088/0256-307X/33/10/106401

It is nowadays a well-established fact that plastic deformation of crystalline solids in nature exhibits an intermittent dynamics in the form of discrete strain avalanches or burst slips. This complex behavior can be found in experiments on the axial compression of micron and submicron sized crystals.[1−4] Although there is consensus that strain avalanches are characterized by power-law distributions of various magnitudes, its universality, such as scaling exponent, is a topic that continues to receive considerable experimental, numerical and theoretical attention.[1,5−8] Interpreting the results from experiments is difficult due to limited statistical sampling, a very limited time resolution and apparatus' sensitivity.[9,10] Many theoretical works on strain avalanches have been developed, such as the automaton model,[11] renormalization group method,[6] and phase field method.[12] Discrete dislocation dynamic (DDD) methods have also provided fruitful tools for analysis of many aspects of strain avalanche in microscale crystal plasticity.[7,13,14]

Alternatively, there is an important analytical tool that has been almost completely overlooked in the published literature. It has been widely shown that the continuum models of plasticity, such as crystal plasticity or gradient plasticity, are applicable to the crystal plasticity at micron and submicron scales.[15−17] In particular, these theories have successfully explained the size effect or intermittent flow induced by strain avalanches in microcompression tests.[15,18,19] However, few theoretical studies to date have focused on these continuum models to obtain a better understanding of the statistics of strain avalanches at micron and submicron scales.

In this Letter, we propose a continuum crystal plasticity model that minimally reproduces the main experimental observations of micropillar compression. An important advantage of this model is that it is able to provide exact quantitative expression of the avalanche size (if a strain avalanche occurs). Furthermore, it provides exact analytical results and quantitative predictions for universal scaling forms, exponents, and functions that can be measured in experiments. These results can be complementary to the microcompression tests or other simulation studies on the mesoscopic level.

We consider the strain avalanche phenomenon of single crystal micropillars at room temperature using a hybrid loading method (HLM).[2] Such a method imposes a nominally constant strain rate $\dot{\varepsilon}_0$, except when the cumulative displacement exceeds the imposed value, such as within a strain avalanche during which the load is kept to be constant. We shall mention that the avalanche-characterized plastic flow in general includes three distinct parts: strain avalanche (burst slip), holding stage, and loading stage.[16] Therefore, the occurrence of strain avalanche in this work evolves from the holding stage (nearly static) or the loading stage (synchronous with the preprogrammed displacement of the indention platen). For further details, see Ref. [16].

To measure the avalanche size accurately, a conservative threshold velocity $V_{\rm th}$ is set. We denote the start of an avalanche when the plate velocity first exceeds $V_{\rm th}$, and its end when the displacement velocity subsequently drops below this threshold. In this way, the strain avalanche is characterized by the starting time $t_{\rm start}$, ending time $t_{\rm end}$, and avalanche velocity $V_{\rm b}(t)$, which is a function of t at which $t_{\rm start} \leq t \leq t_{\rm end}$.[1] For all t within $t_{\rm start} < t < t_{\rm end}$, the avalanche velocity $V_{\rm b}(t)$ satisfies

$$V_{\rm b}(t) > V_{\rm th}, \quad \text{for} \quad t_{\rm start} < t < t_{\rm end}, \tag{1}$$

where $V_{\rm th}$ is usually defined as the mean displacement rate in experiments, or pre-programmed velocity

*Supported by the China Postdoctoral Science Foundation under Grant No 2015M572118, the Outstanding Young Talent Research Fund of Zhengzhou University under Grant No 1521327001, and the National Natural Science Foundation of China under Grant No 51405452.

**Corresponding author. Email: xuzhang@zzu.edu.cn

© 2016 Chinese Physical Society and IOP Publishing Ltd

(by the nanoindentation system) in theories or simulations. It is worth noting that a strain avalanche occurs with sudden jump strain rate. Thus the burst velocity at the beginning time $t_{\rm start}$ can be properly characterized by

$$V^-(t_{\rm start}) \le V_{\rm th}, \quad V^+(t_{\rm start}) > V_{\rm th}, \tag{2}$$

where we suggest that the displacement velocity for the avalanche jump from $V^-(t_{\rm start})$ to $V^+(t_{\rm start})$ at time $t_{\rm start}$. Thus $V^+(t_{\rm start})$ is the jump velocity of the strain avalanche, and $V^-(t_{\rm start})$ represents the displacement velocity in the loading stage or holding stage during the plastic flow. More specifically, we set the displacement rate of $V^-(t_{\rm start}) = V_{\rm th}$ for a loading stage and $V^-(t_{\rm start}) = 0$ for a holding stage. For the strain avalanche at the ending time $t_{\rm end}$, its displacement velocity should satisfy

$$V_{\rm b}(t_{\rm end}) = V_{\rm th}. \tag{3}$$

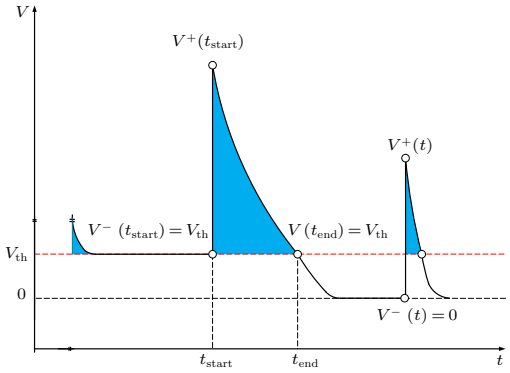

Fig. 1. Schematic drawing of micropillar displacement velocity versus time in the course of plastic flow. The light blue part truncated by $V_{\rm th}$ represents the strain avalanche, which begins at time $t_{\rm start}$ and ends at time $t_{\rm end}$. The curve part that suggests $V = V_{\rm th}$ denotes the loading stage, while the part that V becomes smaller than $V_{\rm th}$ and approaches to zero is the holding stage.

We discuss the avalanche size S in terms of the shear strain. Since the strain avalanche is usually dominated by a single-slip system in single-crystal micropillar plasticity,[13] its size can be properly defined as $S = \frac{A}{ML}$, where A is the burst displacement along the micropillar axis, M is the Schmid factor, and L is the length of micropillar. This is especially true for the micropillar plasticity under the single-slip condition. Here A is defined as the increase in displacement observed from the start to the end of each avalanche $A = d(t_{\rm start}) - d(t_{\rm end})$, with $d(t)$ being the height of micropillar as a function of time.

A simple crystal plasticity model is proposed to reproduce a series of strain avalanches of microsized crystals at room temperature. It is noteworthy that intermittency has been mostly observed under single-slip conditions.[7,11,20] Following that, the present crystal plasticity model represents a two-dimensional (2D) cross section (x–y plane) of a three-dimensional (3D) single crystal with single-slip geometry. In the following we present some relevant descriptions about the crystal plasticity model that we shall describe in detail in a future publication.

Considering a strain avalanche occurring at time $t_{\rm start}$, the produced shear strain $\delta\gamma$ as a function of elapsed time δt can be calculated by

$$\delta\gamma(\delta t) = [(1-\xi)\dot\gamma^+(t_{\rm start}) + \xi\dot\gamma(t_{\rm start} + \delta t)]\delta t, \ \text{for } 0 \le \delta t \le T_{\rm b}, \tag{4}$$

where ξ is the dimensionless constant, $T_{\rm b}$ is the avalanche duration ($T_{\rm b} = t_{\rm end} - t_{\rm start}$) and $\dot\gamma^+(t_{\rm start})$ represents the jump shear strain rate, which is comparable to the jump avalanche velocity $V^+(t_{\rm start})$ in Fig. 1. Notably, whether a burst activity is to be initiated is determined by both the driving force correlated with the externally applied stress $\tau_{\rm ext}$ and the current resistant strength correlated with the internal stress $\tau_{\rm in}$.[3] In this regard, the jump strain rate $\dot\gamma^+(t_{\rm start})$ at the time $t_{\rm start}$ is phenomenologically assumed to be[16,18,21]

$$\dot\gamma^+(t_{\rm start}) = \dot\gamma_0[\tau_{\rm ext}(t_{\rm start})/\tau_{\rm in}(t_{\rm start})]^{1/m}, \tag{5}$$

where $\dot\gamma_0$ is the shear rate at a reference condition, and m is the rate sensitivity exponent. Recent study has shown that the strain burst phenomenon is sensitive to m. Specifically, the value of m increases as the micropillar size decreases.[16]

In Eq. (5), the evolution of $\tau_{\rm ext}$ is given by $\dot\tau_{\rm ext}(t) = E \cdot M[\dot\varepsilon_0 - M\dot\gamma(t)]$, where E is the elastic modulus, and $\dot\varepsilon_0$ is the applied constant strain rate by the nanoindentation system. We shall mention that the avalanche phenomena investigated here are limited to the micron and submicron sized crystals. Therefore, the evolution of flow strength during the plastic deformation is mainly due to the dominance of forest-hardening processes.[22,23] Normally, the phenomenological description of forest hardening process is given by $\dot\tau_{\rm in}(t) = h(t)\dot\gamma^+(t)$, where $h(t)$ is the hardening coefficient as a function of t,[24]

$$h(t) = h_0 {\rm sech}^2\left|\frac{h_0\gamma(t)}{\tau_{\rm s} - \tau_0}\right|, \tag{6}$$

where h_0 is the initial hardening modulus, τ_0 is the initial critical resolved shear stress, and $\tau_{\rm s}$ is the saturated shear stress.

Using the Taylor expansion of $\dot\gamma(t_{\rm start} + \delta t)$ in Eq. (4), we obtain the avalanche size as

$$\delta\gamma(\delta t) = \frac{\left(1 + \frac{\xi\delta\tau_{\rm ex}}{m\tau_{\rm ex}(t_{\rm start})}\right)\dot\gamma^+(t_{\rm start})}{1 + \frac{h(t)\xi}{m\tau_{\rm in}(t_{\rm start})}\dot\gamma^+(t_{\rm start})\delta t}, \tag{7}$$

for $0 \le \delta t \le T_{\rm b}$. Under the condition of HLM, the applied force is kept fixed during a strain avalanche, and thus we obtain $\delta\tau_{\rm ex} \approx 0$. In this way, Eq. (7) can then be rewritten as

$$\delta\gamma(\delta t) = \frac{m\tau_{\rm in}(t_{\rm start})\dot\gamma^+(t_{\rm start})\delta t}{m\tau_{\rm in}(t_{\rm start}) + \dot\gamma^+(t_{\rm start})h(t_{\rm start})\xi\delta t}. \tag{8}$$

According to this equation, the instantaneous shear strain rate is calculated by $\dot\gamma = \frac{d(\delta\gamma)}{d(\delta t)}$ for all t within

$t_{\rm start} < t \leq t_{\rm end}$. Here the ending time of the avalanche is flagged as $t_{\rm end}$ when $\dot{\gamma}$ is truncated by $\dot{\gamma}_{\rm th}$ that is related to $V_{\rm th}$ by $\dot{\gamma}_{\rm th} = \frac{V_{\rm th}}{LM}$. In this case, the effective time step of the strain avalanche is obtained using $T_{\rm b} = t_{\rm start} - t_{\rm end}$. Therefore, the instantaneous shear strain rate in the case of $\delta t = T_{\rm b}$ is

$$\frac{d(\delta\gamma)}{d(\delta t)}\Big|_{\delta t = T_{\rm b}} = \dot{\gamma}_{\rm th}, \tag{9}$$

and we obtain the avalanche size

$$S(t_{\rm start}) = \frac{m\tau_{\rm in}(t_{\rm start})(\kappa - 1)}{\xi h(t_{\rm start})\kappa}, \tag{10}$$

where $\kappa = \sqrt{\frac{\dot{\gamma}^{+}(t_{\rm start})}{\dot{\gamma}_{\rm th}}}$. This equation provides a quantitative description of avalanche size in the crystal plasticity at micron and submicron scales.

For the numerical implementation of the model, we need to treat the statistics of strain increment $\Delta\varepsilon_{\rm l}$ (for the loading stage). However, to our knowledge, the statistics of $\Delta\varepsilon_{\rm l}$ has rarely been studied due to experimental complexity. Here we assume that $\Delta\varepsilon_{\rm l}$ follows approximately an $F(r, s)$ distribution with degrees of freedom r and s, and in this context we expect power-law distributed strain avalanches, as described in the following calculations. Then a hybrid loading procedure is implemented as follows: first, we increase the applied strain ε from zero in small increment $\Delta\varepsilon$, which follows the F distribution. After this strain increment, the shear strain rate $\dot{\gamma}(t)$ is computed by Eq. (5). Then, we check whether $\dot{\gamma}(t)$ is smaller than the threshold value $\dot{\gamma}_{\rm th}$. If it occurs, we will increase the total applied stress by $\Delta\tau_{\rm ext} = E \cdot M[\Delta\varepsilon - M\Delta\gamma]$. If not, a burst slip will occur, and the total external stress keeps to be constant with $\Delta\tau_{\rm ext}(\Delta\varepsilon) = 0$. At every state of strain avalanche, we obtain the avalanche size S from Eq. (10). In the following we study the avalanche size in the context of discrete strain avalanches in micropillar plasticity.

We first verify the rationality of the model by simulating the quasi-compression of Ni pillars of 20 μm diameter.[25] Specifically, the loading is performed with a nominal axial strain rate of 1.0×10^4/s, and the single-slip with a [269] orientation is selected (for this orientation we obtain $E = 221$ GPa and $M = 0.48$). In the computations, $r = 1$ and $s = 4$ are selected for the $F(r, s)$ distribution. A stress-strain curve obtained from this model is shown in Fig. 2. From this plot, the following observations can be made: (i) The increase of plastic strain with increasing the stress occurs in discrete strain avalanches, which are visible as steps on the stress-strain curves. Such steps are admitted to be strain avalanches due to their higher strain rates.[16] (ii) The lengths of steps vary within a certain range, suggesting a stochastic nature of avalanche sizes. (iii) The characteristic avalanche size diverges as one approaches the yield stress. This indicates that the expected avalanche size $S_{\rm max}$ would be reached when the applied stress approaches to the yield stress, in qualitative agreement with the mean-field model.[1,6] (iv) The predicted stress-strain behavior is almost comparable with the experiments (see the inset of Fig. 2). We shall mention that it is difficult for the simulated stress-strain responses to be identical to the experimental observations due to the statistics of strain avalanches.

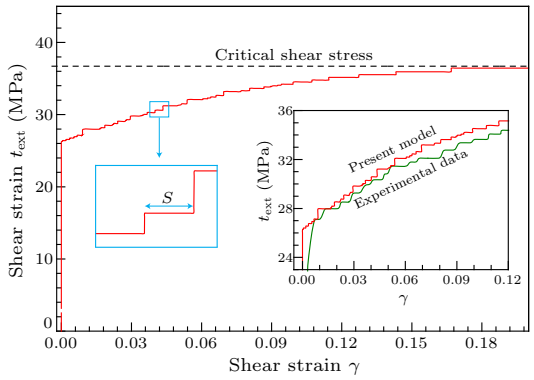

Fig. 2. Shear stress as a function of shear strain for the Ni pillar of ∼20 μm diameter. The avalanche size diverges as one approaches to the critical shear stress $\tau_{\rm c} = 36.5$. The calculations have been carried out for the following parameters: $\xi = 0.2$, $m = 0.003$ and $\dot{\gamma}_0 = 0.001$.[21] The hardening parameters (h_0, τ_0 and $\tau_{\rm s}$) have been discussed in Refs. [16,21]. The inset shows the comparison of shear stress versus strain responses between the simulation and experiment.[25] Here we just show that the theoretical predictions by the present model agree well with the experimental observations.

We now turn our attention to the statistics of avalanche sizes calculated from Eq. (10). Figure 3 shows the probability density distributions of avalanche sizes as obtained from the Ni pillars of ∼20 μm and ∼10 μm diameters. The data in the plot are collected for all stress values. Each specimen size exhibits its probability density distribution for two date sets: a single sample and the aggregate data from multiple samples. Across all simulated samples, the plot clearly shows that the probability density functions of the avalanche size S exhibit power-law decay,

$$P(S) \propto S^{-\tau} f(S/S_0), \tag{11}$$

which is truncated at a characteristic avalanche size S_0 due to finite size effects. The predicted scaling function is in accordance with those derived from the experimental observations[9,26] and DDD simulations,[13] thus suggesting a universal feature.

To estimate the exponent τ and cut-off $f(S/S_0)$, a fitting procedure has been used, which fits Eq. (11) simultaneously to the avalanche distributions obtained at different sizes and data sets. According to the data in a regime featured with cut-off effects, the cut-off is found to follow $f(S/S_0) \propto \exp[-(S/S_0)^{3/2}]$, which again compares well with tail in the avalanche size distributions that are obtained from experimental observations[9,26] and DDD simulations.[13] Figure 3 also shows the collapse with the power-law exponent $\tau = 0.94$, which are smaller than ~ 1.35 that from a recent reanalysis of experimental micropillar compression data[27] and the DDD model.[13] Despite such a discrepancy, the present theoretical predictions

are suggestive of the scaling behaviors from microcompression tests,[1,3,5,9,26] DDD simulations[7,13] and the mean-field theory.[6]

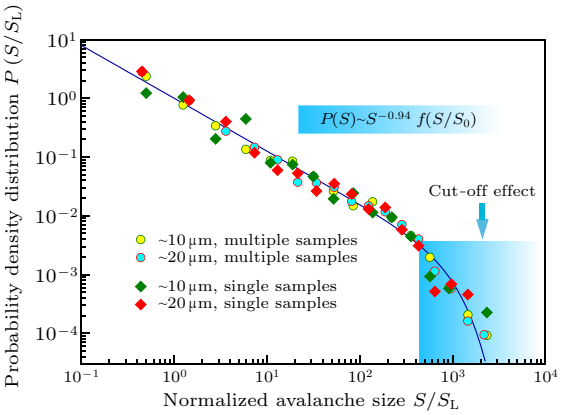

Fig. 3. Probability density distributions of avalanche sizes for the Ni pillars of ∼10 μm and ∼20 μm diameters. The distributions are plotted as a function of S/S_L, where S_L is defined as $S_L = \frac{b}{ML}$ (b is the burgers vector). Note that y-axes of probability density distributions are scaled from original dates, respectively. The solid line reveals the power-law scaling with a cut-off, $S^{-\tau} f(S/S_0)$, which is exhibited for both single sample having ∼10 μm (or ∼20 μm) in diameter (solid circles) and the aggregate data from multiple samples (solid rhombus).

One possible explanation for the low exponent τ may be related to the fact that the real plastic deformation of microcompression in three dimensions and their behaviors are different from the idealized 2D model with single-slip geometry. We shall mention that the present 2D model does not consider the effects of interactions between the glide systems, and thus ignore the hardening of inactive slip systems due to active slip systems. However, it is known that the exponent τ may be affected by the hardening properties.[1] In practice, we find that in our computations, τ becomes larger as the initial hardening modulus h_0 increases. This leads to a reduction of avalanche size and thus an increase of the power-law exponent.[13] Note that h_0 increases as the sample size decreases, as observed in microcompression tests.[28] According to our model, the exponent τ derived from those compressions of larger micropillar would be generally smaller than those derived from nanopillar compressions, consistent with the predictions of the modified MFT model including hardening.[1] That is the reason why we obtain the low exponent τ from the simulated micropillars in 10 μm or 20 μm diameter, with the behaviors more akin to that of bulk metal crystals and displaying more apparent hardening properties.[23] This further suggests that the exponents of power-law distributed strain avalanche may not belong to the universality class.

In conclusion, this study develops a continuum crystal plasticity model that is able to minimally reproduce the main experimental observations of micropillar compression. Although our model is simple, it provides exact analytical results and quantitative predictions for scaling functions and exponents of the avalanche size probability distributions. It is shown that the predicted scaling functions are the same as that derived from the DDD models and experimental observations, suggesting the universal nature of the scaling functions in crystal plasticity. We also suggest that the scaling exponents of strain avalanches may lack universality. While the present 2D model is generally valid for a quantitative characterization of strain avalanche, a 3D continuum crystal plasticity models accounting for the multiple activated-slip-systems are required to better understand the strain avalanches.

References

[1] Friedman N, Jennings A T, Tsekenis G, Kim J K, Tao M, Uhl J T, Greer J R and Dahmen K A 2012 *Phys. Rev. Lett.* **109** 095507
[2] Uchic M D and Dimiduk D M 2005 *Mater. Sci. Eng.* A **400** 268
[3] Maaß R, Derlet P M and Greer J R 2015 *Small* **11** 341
[4] Wang Z J, Li Q J, Shan Z W, Li J, Sun J and Ma E 2012 *Appl. Phys. Lett.* **100** 071906
[5] Maaß R, Derlet P M and Greer J R 2015 *Phys. Rev.* E **91** 042403
[6] Dahmen K A, Ben-Zion Y and Uhl J T 2009 *Phys. Rev. Lett.* **102** 175501
[7] Ispánovity P D, Laurson L, Zaiser M, Groma I, Zapperi S and Alava M J 2014 *Phys. Rev. Lett.* **112** 235501
[8] Weiss J, Rhouma W B, Richeton T, Dechanel S, Louchet F and Truskinovsky L 2015 *Phys. Rev. Lett.* **114** 105504
[9] Papanikolaou S, Dimiduk D M, Choi W, Sethna J P, Uchic M D, Woodward C and Stefano Z 2012 *Nature* **490** 517
[10] Budrikis Z, Fernandez-Castellanos D, Sandfeld S, Zaiser M and Zapperi S 2015 arXiv:1511.06229 [cond-mat.mtrl-sci]
[11] Salman O U and Truskinovsky L 2011 *Phys. Rev. Lett.* **106** 175503
[12] Koslowski M, LeSar R and Thomson R 2004 *Phys. Rev. Lett.* **93** 125502
[13] Csikor F F, Motz C, Weygand D, Zaiser M and Zapperi S 2007 *Science* **318** 251
[14] Cui Y N, Liu Z L and Zhuang Z 2013 *Chin. Phys. Lett.* **30** 046103
[15] Husser E, Lilleodden E and Bargmann S 2014 *Acta Mater.* **71** 206
[16] Zhang X and Shang F L 2014 *Int. J. Solids Struct.* **51** 1859
[17] Liu Z L, Liu X M, Zhuang Z and You X C 2009 *Int. J. Plast.* **25** 1436
[18] Zhang X and Shang F L 2014 *Chin. Phys. Lett.* **31** 026401
[19] Lin P, Liu Z L, Cui Y N and Zhuang Z 2015 *Int. J. Solids Struct.* **69** 267
[20] Ispánovity P D, Groma I, Györgyi G, Csikor F F and Weygand D 2010 *Phys. Rev. Lett.* **105** 085503
[21] Zhang X, Shang F L, Yu Y, Yan Y B and Yan S P 2014 *Int. J. Solids Struct.* **51** 4519
[22] Cui Y N, Lin P, Liu Z L and Zhuang Z 2014 *Int. J. Plast.* **55** 279
[23] Norfleet D M, Dimiduk D M, Polasik S J, Uchic M D and Mills M J 2008 *Acta Mater.* **56** 2988
[24] Peirce D, Asaro R J and Needleman A 1983 *Acta Mater.* **31** 1951
[25] Dimiduk D M, Woodward C, LeSar R and Uchic M D 2006 *Science* **312** 1188
[26] Brinckmann S, Kim J Y and Greer J R 2008 *Phys. Rev. Lett.* **100** 155502
[27] Zhang X, Pan B and Shang F L 2012 *Europhys. Lett.* **100** 16005
[28] Shade P A, Uchic M D, Dimiduk D M, Viswanathan G B, Wheeler R and Fraser H L 2012 *Mater. Sci. Eng.* A **535** 53